PCCP

Accepted Manuscript

ROYAL SOCIETY OF CHEMISTRY

www.rsc.org/pccp

Mechanisms of Peptide hydrolysis by Aspartyl and Metalloproteases

Thomas J. Paul,[†] Arghya Barman,[§] Mehmet Ozbil,[‡] Ram Prasad Bora,[Δ] Tingting Zhang,[⊗]

Gaurav Sharma,[†] Zachary Hoffmann[†] and Rajeev Prabhakar[†]*

Department of Chemistry, University of Miami, 1301 Memorial Drive, Coral Gables, Florida, 33146, USA

Present Address:

[†] *Department of Chemistry, University of Miami, Coral Gables, FL 33146*

[§] *Department of Chemistry, Georgia State University, Atlanta, GA 30302-3965*

[‡] *İstanbul Arel Üniversitesi, Istanbul, Turkey*

[Δ] *Department of Chemistry, University of Southern California, Los Angeles, CA 90089-1062*

[⊗] *Southern Medical University, Guangzhou city, China*

* To whom correspondence should be addressed; rpr@miami.edu; Tel: 305-284-9372; Fax: 305-284-4571.

Abstract: Peptide hydrolysis has been involved in a wide range of biological, biotechnological, and industrial applications. In this perspective, mechanisms of three distinct peptide bond cleaving enzymes, beta secretase (BACE1), insulin degrading enzyme (IDE), and bovine lens leucine aminopeptidase (BILAP) have been discussed. BACE1 is a catalytic Asp dyad [Asp, Asp^-] containing aspartyl protease, while IDE and BILAP are mononuclear [Zn(His, His, Glu)] and binuclear [Zn1(Asp, Glu, Asp)-Zn2(Lys, Glu, Asp, Asp)] core possessing metallopeptidases, respectively. Specifically, enzyme-substrate interactions and the roles of metal ion(s), ligand environment, second coordination shell residues, and protein environment in the functioning of these enzymes have been elucidated. This information will be useful to design small inhibitors, activators, and synthetic analogues of these enzymes for biomedical, biotechnological, and industrial applications.

1. Introduction

The selective hydrolysis of the amide bond (-(O=)C-NH-) of proteins and peptides plays critical roles in several key biological functions such as blood coagulation, immune function, bone formation, programmed cell death, and digestion of proteins.[1-3] Due to these roles, this process has been implicated in numerous life-threatening diseases such as diabetes, cancer, high blood pressure, AIDS, and Alzheimer's disease.[4-6] Peptide hydrolysis is also involved in a wide range of biotechnological applications such as protein footprinting,[7] protein engineering,[8] and bioethanol production.[9] In nature, this formidable task is accomplished by specialized enzymes known as proteases or peptidases.[10-13] Additionally, proteases (cleave peptide bonds of proteins and large peptides) or peptidases (break peptide bonds of short peptides) constitute about 60% of all enzymes that are utilized in textile, food, leather, paper, and ethanol production industries.[9] Peptide bonds are extremely stable and exhibit a half-life for hydrolysis of 350-600 years at room temperature and pH = 4-8.[14] There exist more than 500 different proteases in a human body.[15, 16] Based on the mechanism by which these enzymes cleave peptide bonds, they can be classified into six classes: (1) serine proteases, (2) cysteine proteases, (3) threonine proteases, (4) glutamic proteases, (5) aspartyl proteases, and (6) metalloproteases. Enzymes that constitute the first five subfamilies utilize organic functional groups, while the enzymes belonging to the last subfamily commonly use either a mono- or binuclear metal center to hydrolyze their substrates. Furthermore, cysteine, serine, and threonine proteases catalyze proteolysis utilizing mechanisms independent of water, while aspartyl, glutamic, and metalloproteases use water for peptide hydrolysis.[17-21] In this perspective, we will focus on three distinct members of the aspartyl and metalloproteases families; beta secretase (BACE1), insulin degrading enzyme (IDE), and bovine

lens leucine aminopeptidase (BILAP) with particular emphasis on our work in the field. As discussed below, BACE1 and IDE are two critical proteases that have been implicated in Alzheimer's disease (AD).

The active site of BACE1 contains a catalytic Asp dyad [Asp, Asp^-], while the active sites of IDE and BILAP possess a mononuclear $Zn(N_2O)$ [Zn(His, His, Glu)] and binuclear $Zn1(O_4)$-$Zn2(NO_3)$ [Zn1(Asp, Glu, Asp)-Zn2(Lys, Glu, Asp, Asp)] core, respectively (Figure 1). BACE1 is a type I integral membrane protein that catalyzes proteolysis of a large number (~80) of proteins that play critical roles in several cellular and sub-cellular pathways.[22, 23] This enzyme is well known for catalyzing the rate-limiting steps of the generation of Alzheimer amyloid beta (Aβ) peptides.[13, 24, 25] The inhibition of this enzyme has widely been acknowledged as a promising target for the treatment of AD.[26-31] There are 681 crystal structures of aspartyl proteases in the Protein Data Bank and 344 of them are of BACE1. These X-ray structures suggest that the N-terminal domain of BACE1 that is responsible for the activity displays 30% sequence identity to other members of this family such as pepsin, renin, and cathepsin D. The catalytic [Asp, Asp^-] dyad at the active site is also involved in the functioning of the entire family of aspartyl proteases.[32-39] However, IDE is an endometallopeptidase that catalyzes the degradation of several amyloidogenic substrates like insulin, Aβ, amylin, and glucagon.[40] Due to a common link between insulin and Aβ, patients with type 2 diabetes are under an increased risk of AD.[41, 42] Thus, the inhibitors and activators of this enzyme are potential targets for the treatment of diabetes and AD, respectively.[41] The crystal structures and site-directed mutagenesis studies have demonstrated that the [Zn(His, His, Glu)] core containing active site of IDE has also been observed for other members of this family such as thermolysin (TLN) and

carboxypeptidase A.[43-50] On the other hand, a binuclear core [Zn1(Asp, Glu, Asp)-Zn2(Lys, Glu, Asp, Asp)] possessing BILAP is an exometallopeptidase that prefers to hydrolyze a leucine residue located at the N-terminus in a di- or tripeptide sequence, but it is also capable of hydrolyzing other amino acids as well.[51] This enzyme is extremely prevalent and found in humans, animals, bacteria, and plants.[52, 53] BILAP has been implicated in HIV, cancer, cataract, and cystic fibrosis.[54] Due to their structural and catalytic properties, BACE1, IDE, and BILAP serve as model systems to study aspartyl and metalloproteases.[10, 11, 13, 51, 54, 55]

2. Beta Secretase (BACE1)

To date, approximately 344 X-ray structures of BACE1 (apo form and co-crystal with inhibitors) have been resolved. They showed that the N-terminal domain of BACE1 that is responsible for the catalytic activity exhibits 30% sequence identity to other members of this family such as pepsin, renin, and cathepsin D plus possesses a common fold. These structures also confirmed the presence of the catalytic dyad (Asp32 and Asp228) at the center of the active site of BACE1.[56, 57] A conserved water molecule required for the hydrolysis is also located adjacent to the Asp dyad (Figure 2).[58] This dyad has been implicated in the catalytic functioning of the entire family of aspartyl proteases.[5, 20, 59-64] It is enclosed by an anti-parallel hairpin-loop that resembles a flap (Figure 2). This flap plays a crucial role in the gating mechanism that is utilized by most aspartyl proteases.[65-67] According to this mechanism, the flap opens to allow the entry of the substrate into the active site and guides it towards the Asp dyad for hydrolysis. BACE1 cleaves the Met671-Asp672 amide bond of amyloid precursor protein (APP), referred to as wild-type (WT) substrate, at the extracellular space and initiates the formation of Alzheimer Aβ

peptide(s).[26, 28, 29] A double mutant in the N-terminus region of APP (Lys670 → Asn and Met671 → Leu), the Swedish (SW) substrate, has been reported to enhance the activity of BACE1 by sixty-fold.[68, 69] Here, an outstanding issue was whether the preferential binding of the SW-substrate to BACE1 contributes to its increased activity with respect to the WT-substrate.

2.1. BACE1-substrate (WT and SW) interactions

To address this issue, the interactions of BACE1 with the WT- and SW-substrate were investigated using their octapeptide models (Glu-Val-Lys-*Met*-*Asp*-Ala-Glu-Phe and Glu-Val-Asn-*Leu*-*Asp*-Ala-Glu-Phe, respectively) through all-atom MD simulations.[64] These simulations were performed utilizing the OPLS-AA[70, 71] force field in an explicit TIP4P[72] water model using the GROMACS program.[73, 74] They were performed on the four different structures [apo BACE1, WT-BACE1, SW-BACE1, and an inhibitor (compound 11 (C11), PDB ID: 2qmg) bound BACE1.[75] The structures derived from MD simulations were validated by comparing the positions of the flap and 10s loop and the orientation and interaction of the inhibitor from the compound C11-BACE1 simulation with the corresponding X-ray structure. Additionally, the computed root mean square deviations (rmsd) and B-factors of the C^{α} atoms were used to confirm the accuracy of the equilibrated structures. It was found that the flap closed around 3 ns in the presence of both WT- and SW-substrate at the active site. However, it periodically opened and closed in the apo form. In the BACE1-WT simulation, interaction between the Glu residue of the substrate and Arg307 of BACE1 was lost and the Glu residue interacted with the Lys residue of the substrate. In a site-directed mutagenesis study, the loss of this interaction was also reported to diminish the enzymatic activity.[76] It is quite remarkable that the loss of this single

Glu-Arg307 interaction was observed in our MD simulations. The extent of the flap closing for both substrates was compared by using three key inter-atomic distances (C^{α}(Thr72)-C^{β}(Asp32), C^{α}(Thr72)-C^{α}(Thr329) and OG1(Thr72)-NH1(Arg235)) and the volume of the active site as parameters. It was found that the flap was more closed and the active site was more confined upon the binding of the SW-substrate in comparison to the WT-substrate. Inside the active site, the SW-substrate formed approximately two times (8-10) more hydrogen bonds than the WT-substrate and the nature of hydrophobic interactions was also different. The structures and positions of the inserts A, D, F, and the 10s loop regions of the enzyme were also substantially different upon the binding of these two substrates. All these structural differences explicitly indicated that, in comparison to the WT-substrate, BACE1 demonstrated greater affinity for the SW-substrate and arranged it in a more bioactive conformation.

2.2. Catalytic mechanism of BACE1

Another major unresolved issue regarding the difference in BACE1 activity towards WT- and SW- substrate was the energetic preference for the hydrolysis of the latter over the former. To study this question, the hydrolysis of both WT- and SW-substrates by BACE1 was investigated using two different computational approaches. In the first approach [pure quantum mechanics (QM)], the most representative structures derived from the BACE1-WT and BACE1-SW MD simulations were utilized to develop pruned models of the enzyme-substrate complexes. These structures were used to investigate mechanisms of hydrolytic cleavage of both substrates through density functional theory (DFT).[64] In this approach, electrostatic and steric effects of the protein surrounding were missing. However, in the second approach [hybrid quantum

mechanics/molecular mechanics (QM/MM)], these effects were incorporated using the two-layer ONIOM method by including the whole protein within models.[77]

BACE1 has been proposed to use a general acid-base mechanism for peptide hydrolysis (Figure 3).[20] This mechanism was initially theoretically studied at the *ab-initio* level using simple models.[78-80] In the last few years it has been investigated for the HIV protease,[5, 59-62] presenilin (PS1),[63] and BACE1[64, 77] using more accurate models of their active sites. The X-ray and neutron diffraction data showed that one of the Asp residues of the catalytic dyad was protonated and the second one was unprotonated.[81-84] In the first step, from the reactant (**I**), the unprotonated Asp228 functioned as a base and abstracted a proton from the neighboring conserved water molecule. The hydroxyl (OH^-) nucleophile created in this process concomitantly attacked the carbonyl carbon of the scissile peptide bond. In this process, Asp32 acted as an acid and in a concerted manner donated its proton to the carbonyl oxygen atom of the peptide bond to create the gem-diol intermediate (**II**). Here, it is quite remarkable that Asp228 (p*Ka* value of a free Asp residue ≈ 4.2) pulled a proton from a water molecule (p*Ka* value of a free water ≈ 14.0) to generate the hydroxyl ion. This process requires significant shifts in the p*Ka* values of Asp228 and the water molecule.[85, 86] Currently, the cause and extent of alterations in these p*Ka* values by the microenvironment of BACE1 are not clear. In **II**, two hydroxyl groups were bound to the carbonyl carbon atom of the peptide bond. According to the DFT calculations, the formation of this intermediate occurred through a barrier of 22.4 kcal/mol and 19.1 kcal/mol for the WT- and SW-substrate, respectively (Figure 4b). From **I**, **II** was 15.9 and 8.2 kcal/mol endothermic for the WT- and SW-substrate, respectively. In comparison to **II,** the barrier for the creation of the oxyanion species [$C(OH)(O^-)$] in this step was found to be higher by 36.4 kcal/mol.[63]

In the next step, both Asp residues switched their roles.[81-83] Asp32 now functioned as a base and pulled a proton from the hydroxyl group (–OH) of **II**. Here, Asp228, that acted as a base in the first step, played the role of an acid by donating its proton to the amide nitrogen atom (-NH) of the scissile peptide bond. This concerted process led to the cleavage of the peptide bond and separated amine ($–NH_2$) and carboxyl (–COOH) terminals (**III**) were generated. In this step, the cleavage of the peptide bond proceeded through a barrier of 17.1 and 9.8 kcal/mol for the WT- and SW-substrate, respectively (Figure 4b). The DFT calculations predicted that the formation of the gem-diol intermediate was the rate-determining step of the entire mechanism for both substrates and the barrier for the SW-substrate was 3.3 kcal/mol lower than the WT-substrate. This barrier (19.1 kcal/mol) was found to be in excellent agreement with the measured barrier (k_{cat} = 2.45 s^{-1}) of ~18.0 kcal/mol for this substrate.[87]

In the hybrid QM/MM approach, the barriers for the generation of the gem-diol intermediate in the first step were reduced by 2.8 and 3.2 kcal/mol (19.6 and 16.1 kcal/mol from the reactant) for the WT- and SW-substrate, respectively (Figure 4b).[77] The gem-diol intermediate for the SW-substrate (10.0 kcal/mol) was also 4.7 kcal/mol lower in energy than for the WT-substrate (14.7 kcal/mol). These changes in the computed energetics were caused by the alterations in the reaction coordinates and microenvironment of the active site and were not due to the long-range structural modifications in the enzyme. In the next step, the barrier for the cleavage of the peptide bond was increased by 4.8 and 8.0 kcal/mol for the WT- and SW-substrate, respectively in the QM/MM calculations (21.9 and 17.2 kcal/mol, respectively from the reactant). The

inclusion of the steric and electrostatic effects of the protein surrounding on the energetics rendered the second step as the rate-determining of the entire mechanism. This result was in line with recent crystallographic[88] and Car-Parrinello MD simulations[61] data on another aspartyl protease, HIV protease, that predicted the cleavage of the peptide bond in the rate-limiting step (barrier = 21.0 kcal/mol). In another QM/MM study, the formation of the gem-diol species in the first step was also reported to occur through a barrier of ca. 20.0 kcal/mol for the Leu-Ala substrate.[60] Our QM/MM energetics were supported by experimental observation[87] suggesting that BACE1 can cleave the SW-substrate more efficiently than the WT-substrate.

3. Insulin degrading enzyme (IDE)

Insulin degrading enzyme (IDE) is a Zn^{2+}-containing metallopeptidase found in bacteria, plants and humans.[89] The X-ray structures of the free and substrate (Aβ40 and Aβ42) bound human IDE enzyme have been resolved at 2.8 Å (PDB ID: 2JG4), 2.1 Å (PDB ID: 2G47) and 2.59 Å (PDB ID: 2WK3) resolution, respectively.[40, 90, 91] IDE contains two functional N- and C- terminal domains (IDE-N and IDE-C, respectively) that are joined by an extended 28 amino acid residue loop. They create a large triangular prism shaped catalytic chamber (35×34×30 $Å^3$ and height 36 Å), Figure 5.[40, 90-93] The internal cavity of IDE-N is mostly negative or neutral, while IDE-C possesses a positive charge.[40, 90, 92] The latter assists with substrate binding, whereas the peptide hydrolysis occurs in the former.[90-92, 94] IDE goes through a transition from a closed state to an open state to allow the entry of the substrates into the catalytic chamber. The interactions of the N-terminal residues of the substrates with a conserved exosite that is located ~30 Å away from the active site induce the necessary conformational changes in the substrates for their effective

degradation.[40, 90, 92, 93] Rather surprisingly, the total volume of the catalytic chamber of IDE is almost half of the volume of its substrates such as Aβ40 and Aβ42. Thus, the dynamics and plasticity of both enzyme and substrate are critical for the formation of an active enzyme-substrate complex.[95]

In substrate (Aβ40 and Aβ42)-bound X-ray structures (PDB ID: 2G47 and 2WK3, respectively), the active site Glu111 was substituted with a Gln and the Zn^{2+} ion was missing in the Aβ40-IDE structure.[40, 91] Additionally, all the cysteine residues were mutated in the Aβ42-bound structure.[91] Furthermore, only two discrete fragments of each substrates (Asp1-Glu3 and Lys16-Asp23 of Aβ40 and Asp1-Glu3 and Lys16-Glu22 of Aβ42) were resolved in these structures.[40, 91] Thus, the secondary structures and interactions of the remaining fragments (Phe4-Gln15 and Val24-Val40 of Aβ40 and Phe4-Gln15 and Val24-Ala42 of Aβ42) inside IDE were not experimentally known. Since it is not easy to resolve a structure of a fully active enzyme in the presence of an actual substrate, the inactive form of IDE was used in these X-ray structures.[40, 91] Despite the availability of the aforementioned experimental data, the binding modes of the full-length Aβ peptides and their interactions inside the catalytic chamber of the fully active enzyme remained elusive.

3.1. IDE-substrate (Aβ40 and Aβ42) interactions

To derive this information, interactions between two full-length substrates (Aβ40 and Aβ42) with the active form of IDE were explored through all-atom classical MD simulations.[96] They were performed using the GROMOS force field 53A5[97] as implemented in the GROMACS

program.[73, 74] The free, Aβ40-, and Aβ42-bound (PDB ID: 2JG4, 2G47 and 2WK3, respectively) X-ray structures of IDE and NMR structures of the full-length Aβ40 (PDB ID: 1AML) and Aβ42 (PDB ID: 1IYT) were used to build the initial models for these simulations. The equilibrated structures accurately reproduced the positioning of Zn-metal center and both fragments of Aβ40 and Aβ42 from the X-ray structures. During the simulations, both Aβ40 and Aβ42 underwent substantial structural changes inside the enzyme. Aβ40 coordinated through a large number of intermolecular interactions in the Glu15-Phe19 and Ala21-Lys28 regions. The N-terminal residues of the substrate also interacted with the exosite residues of the enzyme. The structure of Aβ40 inside IDE was significantly different than the ones derived from our MD simulations in the aqueous solution.[98, 99] In the presence of the two additional residues (Ile41-Ala42) a longer and more hydrophobic Aβ42 interacted differently than Aβ40 with the enzyme. This substrate was observed to be more flexible and associated through a smaller number of hydrogen bonds with the enzyme (17-22) in comparison to Aβ40 (25-30). The hydrogen bonding in IDE-Aβ42 complex was less preserved and Aβ42 remained mostly in a disordered random coil formation inside IDE. These MD simulations showed that the length and the chemical nature of the substrate and the environment inside the cavity of the enzyme influence the dynamics and plasticity of both the enzyme and the substrate.

3.2. Catalytic mechanism of IDE

IDE is known to hydrolyze a wide range of peptide bonds (Val12–His13, His14–Gln15, Phe19–Phe20, Lys28–Gly29, etc.) of the Aβ40 and Aβ42 substrates.[40, 90, 100-103] The sequences around these cleavage sites show no similarity. This enzyme, however, does exhibit some preference for

basic or large hydrophobic amino acid on the carboxyl side of the cleavage site. The mechanism of sequential hydrolysis and energetics of the cleavage of these peptide bonds were not available. To investigate the energetic preference, hydrolysis of three chemically distinct peptide bonds, Lys–Gly (polar-nonpolar), Phe–Phe (nonpolar-nonpolar), and His–Gln (polar-polar), were studied through pure QM approach using pruned models of the active site of IDE.[104] Based on the available experimental and theoretical information, the most plausible mechanism utilized by IDE is shown in Figure 6.[104-106] There were certain common features in the general acid-base mechanism utilized by IDE and BACE1.[105] In the reactant (**I**), the scissile peptide bond was polarized through the coordination between the carbonyl oxygen atom (O^8) of the substrate with the positively charged Zn^{2+} metal ion on IDE. On the other hand, in BACE1 the carbonyl oxygen atom interacted through a hydrogen bond with the protonated Asp32 (Figure 3). Here, the metal bound water molecule ($H^2O^1H^3$) was strongly polarized between the negatively charged Glu111 and the Zn^{2+} cation. This polarization decreased its p*Ka* value from ~14 in solution to ~7.[107, 108] In BACE1, in the absence of a metal ion, the conserved water molecule interacted through three hydrogen bonds with Asp228, Asp32 of the enzyme, and the Met (P1) residue of the substrate. In the first step, similar to Asp228 of BACE1, Glu111 acted as a base and pulled a proton from the Zn^{2+} ion bound water molecule. The hydroxyl ($-O^1H^3$) nucleophile generated in this process attacked the α-carbon (C^6) atom of the scissile peptide bond to form an intermediate (**II**). The computed barrier for this step was 14.3, 18.8, and 22.3 kcal/mol for the Lys-Gly, Phe-Phe, and His-Gln bonds, respectively (Figure 6). This step was found to be the rate-determining in the entire mechanism. In the next step, similar to Asp228 in BACE1, Glu111 interchanged its role to an acid and provided its previously acquired proton to the N^7 atom of the peptide bond with the

instantaneous formation of the oxygen-carbon (O^1-C^6) bond. This concerted process created the gem-diol intermediate (**III**). The formation of the gem-diolate intermediate (**III**) occurred through a barrier of 4.9, 7.8, and 10.2 kcal/mol for Lys-Gly, Phe-Phe, and His-Gln, respectively. In the next step, like Asp32 of BACE1, Glu111 acted as a base and abstracted the proton (H^3) from the metal bound oxygen (O^1) atom. This proton transfer cleaved the C^6-N^7 peptide bond and generated the separated carboxyl ($R\text{-}C^6O^1O^{8-}$) and amine ($R\text{-}N^7H_2$) termini (**IV**). The formation of **IV** was exothermic by 10.8, 15.2, and 8.1 kcal/mol exothermic from the corresponding reactants for Lys-Gly, Phe-Phe, and His-Gln, respectively. Similar to aspartyl proteases, the last two steps of the mechanism could occur in a concerted fashion and directly lead to the formation of **IV**.

The presence of the surrounding enzyme in two layer ONIOM (B3LYP/Amber)[109] calculations of this enzyme substantially lowered the barrier for the first step of the mechanism to 11.1 kcal/mol for the Phe-Phe substrate. These calculations predicted that two outer sphere residues (Arg824 and Tyr831) facilitated the formation of **III** by reducing the barrier by 2.5 kcal/mol for the Phe-Phe case. This result was in line with the site directed mutagenesis experiments that showed that these residues played key roles in the functioning of the enzyme.[40] The computed energetics suggested that the nature of the peptide bond played an important role in the cleavage process. As observed in the case of BACE1, in the presence of the protein surrounding the rate-limiting step of the mechanism was associated with the cleavage of the peptide bond.

4. Bovine lens leucine aminopeptidase (BILAP).

Leucine aminopeptidase (LeuAP) is a binuclear metallopeptidases that is found in bacteria, plants, animals, and humans.[54, 110-112] Several X-ray structures of the free and transition-state-analogue complexes of LeuAP from bovine lens (BILAP) have been resolved.[11, 113-116] The N-terminus domain (residues 1-150) of BILAP provides interactions among different monomers, while the active site is located in the C-terminus domain (residues 151-482).[116] The active site of each monomer contains two Zn^{2+} ions that occupy two co-catalytic sites.[54, 117-120] The Zn^{2+} ion at site 1 (Zn1) is bound to the Asp255, Asp332, and Glu334 residues, while Zn^{2+} ion at site 2 (Zn2) to Lys250, Asp255, Asp273, and Glu334. The Zn1-Zn2 distance at the active site was ≈ 3.02 Å, Figure 1. Both nonequivalent metal binding sites are required for the enzymatic activity.[54] The measured kinetic data using two different substrates L-leucine-*p*-nitroanilide ($NO_2C_6H_4NHCOCH(NH_2)CH_2CH(CH_3)_2$) and L-leucyl-*p*-anisidine ($CH_3OC_6H_4NHCOCH(NH_2)CH_2CH(CH_3)_2$) for the Mg1-Zn2 and Mg1-Co2 variants also showed that k_{cat} depends on the interaction between both metal ions sites.[121] There were several outstanding issues regarding the mechanism of this enzyme. The exact protonation state of the nucleophile (H_2O or -OH) was not clear.[114, 122] The influence of the electronic nature of the substrate (an electron withdrawing nitro group ($-NO_2$) in the L-leucine-*p*-nitroanilide and an electron donating methoxy group ($-OCH_3$) of the L-leucyl-*p*-anisidine) on the structures was not known.[121] The role of each metal center and structures of Mg and Co variants were not available. We investigated all these issues using DFT calculations in the pure QM approach.[123]

4.1 Catalytic mechanism of BILAP

Based on experimental and theoretical data,[51, 114, 122, 123] the most plausible acid/base mechanism proposed for the hydrolysis of the L-Leu-p-nitroanilide substrate by BILAP is shown in Figure 7. Kinetic isotope experiments and the absence of nucleophilic residues at the active site had ruled out the possibility of an anhydride mechanism involving a covalent intermediate.[124] Since the identity of the nucleophile (water or hydroxide ion) that is bridging both (Zn1 and Zn2) metal ions was not exactly known, this mechanism is generally discussed in the literature using a bridging water molecule. However, in some theoretical studies of other members of this family *Aeromonas proteolytica* aminopeptidase (AAP),[125] methionine aminopeptidase (MetAP),[126] and prolidase[127] a mechanism involving a hydroxyl (-OH) ion in the reactant was used.

In the reactant with the water molecule ($\mathbf{I_W}$), both Zn1 and Zn2 ions existed in the penta-coordinated form with the Zn1-Zn2 distance of 3.18 Å. The Zn1 ion polarized the scissile peptide bond through the formation of a bond with the carbonyl oxygen of the peptide bond, while Zn2 participated in positioning the substrate through interactions with its N-terminus. Additionally, the coordination to both metal centers significantly reduced the p*Ka* value of the water molecule.[128] This mechanism exhibits some common features with the one utilized by mononuclear Zn^{2+} center containing IDE. However, in IDE the water molecule was bound to the only Zn ion. In both BILAP and IDE, one Zn ion is involved in the polarization of the peptide bond through the formation of the metal-oxygen bond. In the first step, a bicarbonate ion functioned as a base and abstracted a proton from the bridging water molecule to create the hydroxyl nucleophile. The hydroxyl ion bound to Zn2 simultaneously attacked the electrophilic carbon atom (C^1) of the peptide bond (C^1-N^2) to form the *gem*-diolate intermediate ($\mathbf{II_W}$). The formation of $\mathbf{II_W}$ occurred with a computed barrier of 18.6 kcal/mol from $\mathbf{I_W}$ (Figure 7a). The

catalytic base bicarbonate ion of BILAP and Glu111 of IDE were located in the second coordination shell. The hydroxyl group bound to two metal centers should be a weaker nucleophile than the one coordinated to the one metal center. Thus, the hydroxyl nucleophile was bound to only one Zn ion in transition states of this step for both IDE and BILAP (Figure 6 and 7a).

In the next step, the bicarbonate ion acted as an acid and donated its proton to the nitrogen atom (N^2) to split the amide bond. However, in IDE the second coordination shell Glu111 residue played the role of acid in this process. Unlike the mechanism of IDE, this process occurred in the rate-limiting step of the mechanism with a computed barrier of 25.5 kcal/mol. The acid/base role played by the bicarbonate ion in this mechanism was similar to the one observed in the catalytic cycle of cyclopropane synthase.[129, 130] The removal of the bicarbonate ion reduced the k_{cat} value by eight-fold and a cluster of three water molecules replaced its function.[122] This substitution was also found to increase the barrier by 4.9 kcal/mol in our DFT calculations. This increase was ~3.7 kcal/mol higher than the one observed experimentally. The B3LYP method used in these calculations has previously been shown to overestimate computed barriers by 3-5 kcal/mol for proton transfer reactions using a chain of water molecules.[131]

From $\mathbf{I_W}$, a proton transfer from the bridging water to the Zn2 bound Asp273 base could generate another reactant ($\mathbf{I_H}$ in Figure 7b). In $\mathbf{I_H}$, the hydroxyl nucleophile was coordinated to both Zn1 and Zn2 ions and protonated Asp273 was bound to the Zn2 ion. This type of reactant has been used in theoretical studies of AAP,[125] MetAP,[126] and prolidase[127] that lack the bicarbonate ion. The $\mathbf{I_H}$ could be created from $\mathbf{I_W}$ with a barrier of 13.5 kcal/mol which was 7.8

kcal/mol higher in energy than the latter. From $\mathbf{I_H}$, the formation of the *gem-diolate* intermediate occurred with a barrier of 10.8 kcal/mol. In the next rate-determining step, the cleavage of the peptide bond took place with a barrier of 17.8 kcal/mol. This barrier was in excellent agreement with the experimentally measured barrier of 18.7 kcal/mol ($k_{cat} \approx 7$ min^{-1}).[121] The substitution of the L-leucine-*p*-nitroanilide substrate with L-leucyl-*p*-anisidine showed that all three steps of the mechanism occurred with similar barriers i.e. 18.7, 19.3, and 18.0 kcal/mol for step 1, step 2, and step 3, respectively. Furthermore, energetics of the Mg1-Zn2 and Mg1-Co2 variants of the enzyme suggested that the nature of the metal ion affect only the formation of the *gem*-diol intermediate in the first step and after that all three variants followed essentially the same energetics.

4.2. Role of active site microenvironment in peptide hydrolysis

To explore the role of microenvironments of the active site, the hydrolysis of a single peptide bond (Phe1-Phe2) by the three types of catalysts was studied: (1) BACE, (2) IDE, and (3) Zn(N_3) [Zn(His, His, His)] core containing matrix metalloproteinase (MMP)].[132] Our DFT calculations allowed us to make the following interesting comparisons: (1) the effect of the active site in two aspartate residues containing aspartyl protease (BACE) and metallopeptidases (MMP and IDE) and (2) the influence of the ligand environment of the Zn^{2+} center in MMP (His, His His (N_3)) and IDE (His, His, Glu (N_2O)). The computed energetics for all three catalysts were in good agreement with the measured and theoretical data.[63, 87, 104, 108, 133-135] They predicted that among these catalysts MMP with [N_3] moiety was the most efficient in catalyzing this reaction (Table 1). BACE and IDE catalyzed this reaction with 5.0 and 6.9 kcal/mol higher

barriers than MMP, respectively. The difference between MMP and IDE could be attributed to the reduction in acidity of the Zn ion in the N_2O moiety of IDE. In a marked contrast from IDE, the rate-limiting step was predicted to be associated with the cleavage of the peptide bond for MMP. The lower barrier for BACE in comparison to IDE was quite surprising.

5. Concluding Remarks and Perspectives.

In this perspective, we have discussed the mechanisms of three critical proteases BACE1, IDE, and BILAP. A plethora of computational chemistry techniques have been employed to gather this information. Our theoretical studies provided structures of short-lived intermediates and transition states and energetics of their catalytic cycles. Additionally, deeper understanding regarding the roles of metal ion(s), ligands, and the microenvironment of the reaction center in the functioning of these enzymes was developed. They also revealed certain common features in the general acid/base mechanisms utilized by these three distinct enzymes. It was found that in the absence of protein surrounding creation of hydroxyl nucleophile from a water nucleophile occurred in the rate-determining step for BACE1 and IDE. However, the inclusion of electronic and steric effects of the protein environment in the calculations lowered the barrier for this step and raised the barrier for the cleavage of peptide bond in the next step for both enzymes. Currently, the information regarding the pK_a shifts, binding affinity of the conserved water molecule, and protonation states of the key active site residues in this process is not consistently available. These details will be required to develop a better understanding of the functioning of these enzymes and to design their inhibitors and activators. They will also be useful in design of synthetic analogues of these enzymes for biotechnological and industrial applications.[136]

Furthermore, the knowledge gained from the studies of peptide hydrolysis may also be useful in designing small molecules that catalyze the hydrolysis of esters, nitriles, phosphates, and other organic reactions including epoxide opening, aldol condensation, Michael addition, and Diels-Alder reactions. However, despite the significant amount of research performed in the last three decades true synthetic analogues of these enzymes are still elusive. Their design will require multidisciplinary efforts involving both theory and experiments in the future.

Acknowledgements

Financial support from the James and Esther King Biomedical Research Program of the Florida State Health Department (DOH grant number 08KN-11) and National Science Foundation (NSF grant number CHE 1152846) to R.P. is greatly acknowledged. Computational resources from the Center for Computational Science (CCS) at the University of Miami are greatly appreciated. The authors also thank Vindi Jayasinghe Arachchige for help with preparation of the manuscript.

References:

1. B. Turk, *Nat. Rev. Drug Discov.*, 2006, 5, 785-799.
2. E. W. Davie and H. Neurath, *J. Biol. Chem.*, 1955, 212, 515-530.
3. E. W. Davie and O. D. Ratnoff, *Science*, 1964, 145, 1310-1312.
4. D. R. Davies, *Annu. Rev. Biophys. Biophys. Chem.*, 1990, 19, 189-215.
5. S. Bjelic and J. Åqvist, *Biochemistry*, 2006, 45, 7709-7723.
6. D. J. Selkoe, *Physiol. Rev.*, 2001 81, 741-766.
7. N. Baichoo and T. Heyduk, *Prot. Sci.*, 1999, 8, 518-528.

8. C. J. A. Wallace, *Protein Engineering by Semisynthesis*, CRC Press, Boca Raton, Fl., 2000.

9. Y. M. Galante and C. Formantici, *Curr. Org. Chem.*, 2003, 7, 1399-1422.

10. B. M. Dunn, *Chem. Rev.*, 2002, 102, 4431-4458.

11. W. N. Lipscomb and N. Sträter, *Chem. Rev.*, 1996, 96, 2375-2434.

12. L. Tong, *Chem. Rev.*, 2002, 102, 4609-4626.

13. M. S. Wolfe, *Chem. Rev.*, 2009, 109, 1599-1612.

14. A. Radzicka and R. Wolfenden, *J. Am. Chem. Soc.*, 1996, 118, 6105-6109.

15. L. M. S. X.S. Puente, A. Gutiérrez-Fernández, G. Velasco and C. López-Otín, *Biochem. Soc. Trans.*, 2005, 33, 331–334

16. N. D. Rawlings, M. Waller, A. J. Barrett and A. Bateman, *Nucleic Acids Res*, 2014, 42, 503-509.

17. J. C. Powers, J. L. Asgian, Ö. D. Ekici and K. E. James, *Chem. Rev.*, 2002, 102, 4639-4750.

18. L. Hedstrom, *Chem. Rev.*, 2002, 102, 4501-4524.

19. G. Dodson and A. Wlodawer, *TIBS*, 1998, 23, 347-352.

20. K. Suguna, E. A. Padlan, C. W. Smith, W. D. Carlson and D. R. Davies, *Proc. Natl. Acad. Sci. USA*, 1987, 84, 7009-7013.

21. A. Brik and C.-H. Wong, *Org. Biomol. Chem.*, 2003, 1, 5-14.

22. F. Grüninger-Leitch, D. Schlatter, E. Küng, P. Nelböck and H. Döbeli, *J. Biol. Chem.*, 2002, 277, 4687-4693.

23. M. L. Hemming, J. E. Elias, S. P. Gygi and D. J. Selkoe, *PLoS ONE*, 2009, 4, e8477.

24. G. Thinakaran and E. H. Koo, *J. Biol. Chem.*, 2008, 283, 29615-29619.

25. M. S. Wolfe, W. Xia, C. L. Moore, D. D. Leatherwood, B. Ostaszewski, T. Rahmati, I. O. Donkor and D. J. Selkoe, *Biochemistry*, 1999, 38, 4720-4727.

26. R. Yan, M. E. Bienkowski, M. E. Shuck, H. Miao, M. C. Tory, A. M. Pauley, J. R. Brashler, N. C. Stratman, W. R. Mathews, A. E. Buhl, D. B. Carter, A. G. Tomasselli, L. A. Parodi, R. L. Heinrikson and M. E. Gurney, *Nature*, 1999, 402, 533-537.

27. J. Hardy, *Trends Neurosci.*, 1997, 20, 154-159.

28. R. Vassar, B. D. Bennett, S. Babu-Khan, S. Kahn, E. A. Mendiaz, P. Denis, D. B. Teplow, S. Ross, P. Amarante, R. Loeloff, Y. Luo, S. Fisher, J. Fuller, S. Edenson, J. Lile, M. A. Jarosinski, A. L. Biere, E. Curran, T. Burgess, J. C. Louis, F. Collins, J. Treanor, G. Rogers and M. Citron, *Science*, 1999, 286, 735-741.

29. S. Sinha, J. P. Anderson, R. Barbour, G. S. Basi, R. Caccavello, D. Davis, M. Doan, H. F. Dovey, N. Frigon, J. Hong, K. Jacobson-Croak, N. Jewett, P. Keim, J. Knops, I. Lieberburg, M. Power, H. Tan, G. Tatsuno, J. Tung, D. Schenk, P. Seubert, S. M. Suomensaari, S. Wang, D. Walker, J. Zhao, L. McConlog and V. John, *Nature*, 1999, 402, 537-540.

30. H. Cai, Y. Wang, D. McCarthy, H. Wen, D. R. Borchelt, D. L. Price and P. C. Wong, *Nat Neurosci*, 2001, 4, 233-234.

31. Y. Luo, B. Bolon, S. Kahn, B. D. Bennett, S. Babu-Khan, P. Denis, W. Fan, H. Kha, J. Zhang, Y. Gong, L. Martin, J.-C. Louis, Q. Yan, W. G. Richards, M. Citron and R. Vassar, *Nat Neurosci*, 2001, 4, 231-232.

32. D. C. Chatfield, K. P. Eurenius and B. R. and Brooks, *J. Mol. Struct.: THEOCHEM*, 1998, 423, 79-92.

33. K. Suguna, E. A. Padlan, C. W. Smith, W. D. Carlson and D. R. and Davies, *Proc. Natl. Acad. Sci. USA*, 1987, 84, 7009-7013.

34. M. Cascella, C. Micheletti, U. Rothlisberger and P. and Carloni, *J. Am. Chem. Soc.*, 2005, 127, 3734-3742.

35. S. Bjelic and J. Åqvist, *Biochemistry*, 2006, 45, 7709-7723.

36. S. Piana, D. Bucher, P. Carloni and U. and Rothlisberger, *J. Phys. Chem. B*, 2004, 108, 11139-11149.

37. J. Trylska, P. Grochowski and J. A. McCammon, *Protein Sci.*, 2004, 13, 513-528.

38. R. Singh, A. Barman and a. P. R., *J. Phys. Chem. B*, 2009, 113, 2990-2999.

39. A. Barman, S. Schürer and R. and Prabhakar, *Biochemistry*, 2011, 50, 4337-4349.

40. Y. Shen, A. Joachimiak, M. R. Rosner and W. J. Tang, *Nature*, 2006, 443, 870-874.

41. W. Q. Qiu and M. F. Folstein, *Neurobiol. Aging*, 2006, 27, 190-198.

42. G. Taubes, *Science*, 2003, 301, 40–41.

43. H. Im, Manolopoulou, M., Malito, E., Shen, Y., Zhao, J., Neant-Fery, M., Sun, C-Y, Meredith, S. C., Sisodia, S. S., Leissering, M. A., and Tang, W-J., *J. Biol. Chem.*, 2007, 282, 25453-25463.

44. Y. Shen, Joachimiak, A., Rosner, M. R., and Tang, W-J., *Nature*, 2006, 443, 870-874.

45. A. B. Becker, and Roth, R. A., *Proc. Natl. Acad. Sci.*, 1992, 89, 3835-3839.

46. R. K. Perlman, and Rosner, M. R., *J. Biol. Chem*, 1994, 269, 33140–33145.

47. B. W. Matthews, Jansonius, J.N., Colman, P.M., Schoenborn, B.P., and Dupourque, D., *Nature*, 1972, 238, 37-41.

48. D. R. Holland, Hausrath, A. C., Juers, D., and Matthews, B. W., *Protein Sci.*, 1995, 4, 1955-1965.

49. F. A. Quiocho, C. H. McMurray and W. N. Lipscomb, *Proc. Natl. Acad. Sci. USA*, 1972, 69, 2850-2854.

50. B. W. Matthews, Schoenbo.Bp, Dupourqu.D, Jansoniu.Jn and P. M. Colman, *Nature-New Bio.*, 1972, 238, 37.

51. W. T. Lowther and B. W. Matthews, *Chem. Rev.*, 2002, 102, 4581 - 4608.

52. J. Weston, *Chem. Rev.*, 2005, 105, 2151-2174.

53. D. E. Wilcox, *Chem. Rev.*, 1996, 96, 2435-2458.

54. A. Taylor, *FASEB J.*, 1993, 7, 290-298.

55. B. L. Vallee and D. S. Auld, *Biochemistry*, 1993, 32, 6493-6500.

56. L. Hong, G. Koelsch, X. Lin, S. Wu, S. Terzyan, A. K. Ghosh, X. C. Zhang and J. Tang, *Science*, 2000, 290, 150-153.

57. L. Hong, R. T. Turner III, G. Koelsch, G. Shin, A. K. Ghosh and J. Tang, *Biochemistry*, 2002, 41, 10963-10967.

58. N. S. Andreeva and L. D. Rumsh, *Protein Sci.*, 2001, 10, 2439-2450.

59. D. C. Chatfield, K. P. Eurenius and B. R. Brooks, *J. Mol. Struct.: THEOCHEM*, 1998, 423, 79-92.

60. M. Cascella, C. Micheletti, U. Rothlisberger and P. Carloni, *J. Am. Chem. Soc.*, 2005, 127, 3734-3742.

61. S. Piana, D. Bucher, P. Carloni and U. Rothlisberger, *J. Phys. Chem. B*, 2004, 108, 11139-11149.

62. J. Trylska, P. Grochowski and J. A. McCammon, *Prot. Sci.*, 2004, 13, 513-528.

63. R. Singh, A. Barman and R. Prabhakar, *J. Phys. Chem. B*, 2009, 113, 2990-2999.

64. A. Barman, S. Schürer and R. Prabhakar, *Biochemistry*, 2011, 50, 4337-4349.

65. H. Shimizu, A. Tosaki, K. Kaneko, T. Hisano, T. Sakurai and N. N, *Mol. Cell. Biol.*, 2008, 28, 3663-3671.

66. F. Pietrucci, F. Marinelli, P. Carloni and A. Laio, *J. Am. Chem. Soc.*, 2009, 131, 11811-11818.

67. W. R. P. Scott and C. A. Schiffer, *Structure*, 2000, 8, 1259–1265.

68. M. Citron, T. S. Diehl, G. Gordon, A. L. Biere, P. Seubert and D. J. Selkoe, *Proc. Natl. Acad. Sci. USA*, 1996, 93, 13170-13175.

69. X. D. Cai, T. E. Golde and S. G. Younkin, *Science*, 1993, 259, 514-516.

70. W. L. Jorgensen and J. Tirado-Rives, *J. Am. Chem. Soc.*, 1988, 110, 1657-1666.

71. G. A. Kaminski, R. A. Friesner, J. Tirado-Rives and W. L. Jorgensen, *J. Phys. Chem. B*, 2001, 105, 6474-6487.

72. W. Jorgensen, L., , J. Chandrasekhar, J. Madura, D., , R. Impey, W., and M. Klein, L., *J. Chem. Phys.*, 1983, 79, 926-935.

73. H. J. C. Berendsen, D. van der Spoel and D. van Drunen, *Comput. Phys. Commun.*, 1995, 91, 43-56.

74. E. Lindahl, B. Hess and D. van der Spoel, *J. Mol. Model.*, 2001, 7, 306-317.

75. U. Iserloh, Y. Wu, J. N. Cumming, J. Pan, L. Y. Wang, A. W. Stamford, M. E. Kennedy, R. Kuvelkar, X. Chen, E. M. Parker, C. Strickland and J. Voigt, *Bioorg. Med. Chem. Lett.*, 2008, 18, 414-417.

76. R. T. Turner, G. Koelsch, L. Hong, P. Castenheira, A. Ghosh and J. Tang, *Biochemistry*, 2001, 40, 10001-10006.

77. A. Barman and R. Prabhakar, *J. Mol. Graph. Model.*, 2013, 40, 1-9.

78. M. Strajbl, J. Florian and A. Warshel, *J. Am. Chem. Soc.*, 2000, 122, 5354-5366.

79. Z. Wu, F. Ban and R. J. Boyd, *J. Am. Chem. Soc.*, 2003, 125, 6994-7000.

80. H. Park, J. Suh and S. Lee, *J. Am. Chem. Soc.*, 2000, 122, 3901-3908.

81. L. Coates, P. Erskine, S. Mall, R. Gill, S. Wood, D. Myles and J. Cooper, *Eur. Biophys. J.*, 2006, 35, 559-566.

82. L. Coates, H.-F. Tuan, S. Tomanicek, A. Kovalevsky, M. Mustyakimov, P. Erskine and J. Cooper, *J. Am. Chem. Soc.*, 2008, 130, 7235-7237.

83. R. Rajamani and C. H. Reynolds, *J. Med. Chem.*, 2004, 47, 5159 - 5166.

84. N. Yu, S. A. Hayik, B. Wang, N. Liao, C. H. Reynolds and K. M. Merz, *J. Chem. Theory Comput.*, 2006, 2, 1057-1069.

85. C. R. Ellis and J. Shen, *J. Am. Chem. Soc.*, 2015, 137, 9543-9546.

86. C. R. Ellis, C.-C. Tsai, X. Hou and J. Shen, *J. Phys. Chem. Lett.*, 2016, 7, 944-949.

87. X. Lin, G. Koelsch, S. Wu, D. Downs, A. Dashti and J. Tang, *Proc. Natl. Acad. Sci. USA*, 2000, 97, 1456-1460.

88. A. Das, S. Mahale, V. Prashar, S. Bihani, J. L. Ferrer and M. V. Hosur, *J. Am. Chem. Soc.*, 2010, 132, 6366-6373.

89. I. A. Mirsky and R. H. Broth-Kahn, *Arch. Biochem.*, 1949, 20, 1-9.

90. H. Im, M. Manolopoulou, E. Malito, Y. Shen, J. Zhao, M. Neant-Fery, C.-Y. Sun, S. C. Meredith, S. S. Sisodia, M. A. Leissering and W. J. Tang, *J. Biol. Chem.*, 2007, 282, 25453-25463.

91. Q. Guo, M. Manolopoulou, Y. Bian, A. B. Schilling and W. J. Tang, *J. Mol. Biol.*, 2010, 395, 430-443.

92. E. Malito, L. A. Ralat, M. Manolopoulou, J. L. Tsay, N. L. Wadlington and W. J. Tang, *Biochemistry*, 2008, 47, 12822-12834.

93. M. Manolopoulou, Q. Guo, E. Malito, A. B. Schilling and W. J. Tang, *J. Biol. Chem.*, 2009, 284, 14177-14188.

94. P. Li, W. L. Kuo, M. Yousef, M. R. Rosner and W. J. Tang, *Biochem. Biophys. Research Commun.*, 2006, 343, 1032-1037.

95. M. Ozbil, A. Barman, R. P. Bora and R. Prabhakar, *J. Phys. Chem. Lett.*, 2012, 3, 3460-3469.

96. R. P. Bora and R. Prabhakar, *Biochemistry*, 2010, 49 3947–3956.

97. C. Oosteinbrink, A. Villa, A. E. Mark and W. F. van Gunsteren, *J. Comput. Chem.*, 2004, 25, 1656-1676.

98. L. Triguero, R. Singh and R. Prabhakar, *J. Phys. Chem. B*, 2008, 112, 7123-7131.

99. R. P. Bora and R. Prabhakar, *J. Chem. Phys.*, 2009, 131, 155103.

100. E. Malito, R. E. Hulse and W.-J. Tang, *Cell. Mol. Life Sci.*, 2008, 65, 2574-2585.

101. I. Kurochkin and S. Goto, *FEBS Lett*, 1994, 345, 33-37.

102. I. Kurochkin, *Trends Biochem. Sci.*, 2001, 26, 421-425.

103. I. V. Kurochkin, *FEBS Lett*, 1998, 427, 153-156.

104. R. P. Bora, M. Ozbil and R. Prabhakar, *J. Biol. Inorg. Chem.*, 2010, 15, 485-495.

105. D. W. Christianson and W. N. Lipscomb, *Acc. Chem. Res.*, 1989, 22, 62-69.

106. O. Amata, T. Marino, N. Russo and M. Toscano, *J. Am. Chem. Soc.*, 2009, 131, 14804-14811.

107. A. Glades and B. L. Vallee, *Metal ions in biological systems*, Dekker, New York, 1983.

108. V. Pelmenschikov, M. R. A. Blomberg and P. E. M. Siegbahn, *J. Biol. Inorg. Chem.*, 2002, 7, 284-298.

109. S. Dapprich, I. Komaromi, S. Byun, K. Morokuma and J. M. Frisch, *J. Mol. Struct. (Theochem)*, 1999, 461 1-21.

110. N. Sträter, D. J. Sherratt and S. D. Colloms, *EMBO J*, 1999, 18, 4513-4522.

111. I. A. York, A. L. Goldberg, X. Y. Mo and K. L. Rock, *Immunol. Rev.*, 1999, 172, 49-66.

112. M. Matsui, J. H. Fowler and L. L. Walling, *Biol. Chem.*, 2006, 387, 1535-1544.

113. S. K. Burley, P. R. David, R. M. Sweet, A. Taylor and W. N. Lipscomb, *J. Mol. Biol.*, 1992, 224, 113-140.

114. N. Sträter and W. N. Lipscomb, *Biochemistry*, 1995, 34, 14792-14800.

115. H. Kim and W. N. Lipscomb, *Biochemistry*, 1993, 32, 8465-8478.

116. S. K. Burley, P. R. David, A. Taylor and W. N. Lipscomb, *Proc. Natl. Acad. Sci. U. S. A.*, 1990, 87, 6878-6882.

117. S. R. Himmelhoch, *Arch. Biochem. Biophys.*, 1969, 134, 597-602.

118. F. H. Carpenter and J. M. Vahl, *J. Biol. Chem.*, 1973, 248, 294-304.

119. F. H. Carpenter and K. T. Harrington, *J. Biol. Chem.*, 1972, 247, 5580-5586.

120. S. W. Melbye and F. H. Carpenter, *J. Biol. Chem.*, 1971, 246, 2459-2463.

121. M. P. Allen, A. H. Yamada and F. H. Carpenter, *Biochemistry*, 1983, 22, 3778-3783.

122. N. Sträter, L. Sun, E. R. Kantrowitz and W. N. Lipscomb, *Proc. Natl. Acad. Sci. U. S. A.*, 1999, 96, 11151-11155.

123. X. Zhu, A. Barman, M. Ozbil, T. Zhang, S. Li and R. Prabhakar, *J. Biol. Inorg. Chem.*, 2012, 17, 209-222.

124. V. K. Antonov, L. M. Ginodman, L. D. Rumsh, Y. V. Kapitannikov, T. N. Barshevskaya, L. P. Yavashev, A. G. Gurova and L. I. Volkova, *Eur. J. Biochem.*, 1981, 117, 195-200.

125. S.-L. Chen, T. Marino, W.-H. Fang, N. Russo and F. Himo, *J. Phys. Chem. B*, 2008, 112, 2494-2500.

126. M. Leopoldini, N. Russo and M. Toscano, *J. Am. Chem. Soc.*, 2007, 129, 7776-7784.

127. M. E. Alberto, M. Leopoldini and N. Russo, *Inorg. Chem.*, 2011, 50, 3394-3403.

128. J. T. Groves and J. R. Olson, *Inorg. Chem.*, 1985, 24, 2715-2717.

129. C. Huang, C. V. Smith, M. S. Glickman, W. R. Jacobs and J. C. Sacchettini, *J. Biol. Chem.*, 2002, 277, 11559-11569.

130. F. Courtois and O. Ploux, *Biochemistry*, 2005, 44, 13583-13590.

131. R. Prabhakar, A. M. R. Blomberg and M. P. E. Siegbahn, *Theor. Chem. Acc.*, 2000, 104, 461-470.

132. R. P. Bora, A. Barman, X. Zhu, M. Ozbil and R. Prabhakar, *J. Phys. Chem. B*, 2010, 114, 10860–10875.

133. L. Polgar, Z. Szeltner and I. Boros, *Biochemistry*, 1994, 33, 9351-9357.

134. V. Pelmenschikov and P. E. M. Siegbahn, *Inorg. Chem.*, 2002, 41, 5659-5666.

135. K. Morihara and T. Hiroshige, *Eur. J. Biochem.*, 1970, 15, 374-380.

136. T. Zhang, M. Ozbil, A. Barman, T. J. Paul, R. P. Bora and R. Prabhakar, *Acc. Chem. Res.*, 2015, 48, 192-200.

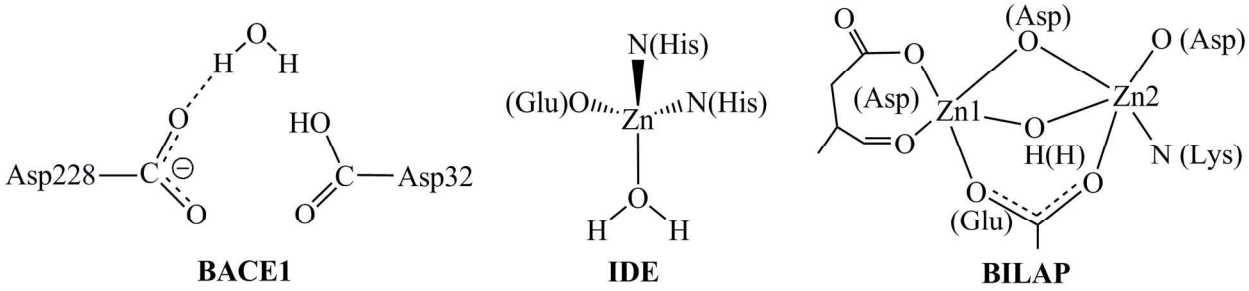

Figure 1: Active sites of three distinct proteases; BACE1, IDE and BILAP

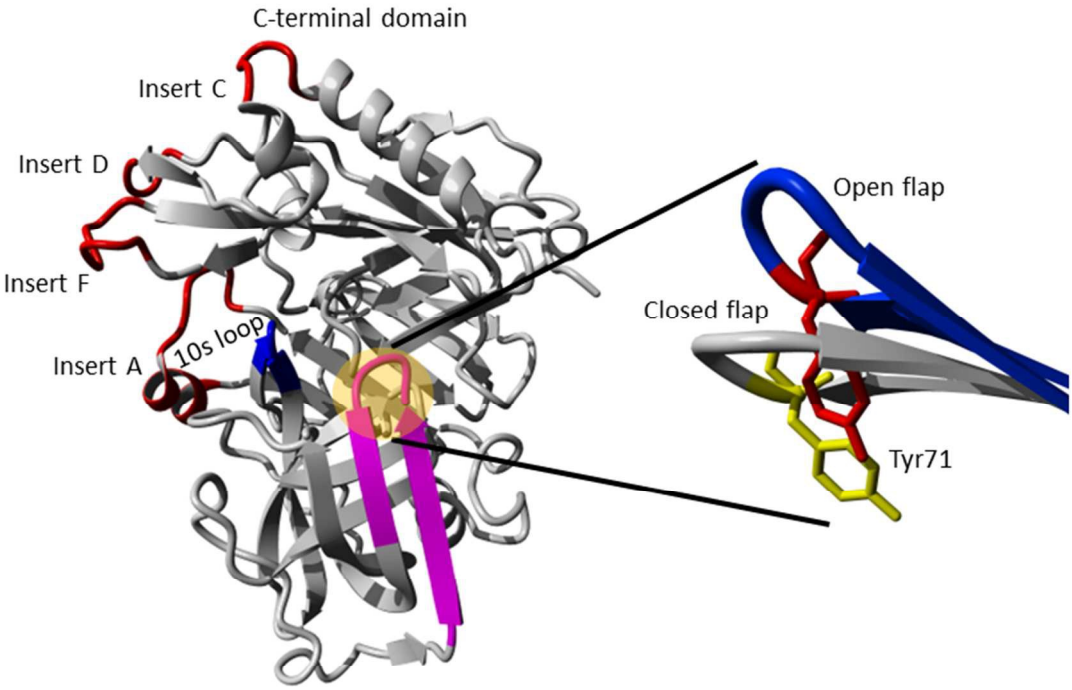

Figure 2: Structures of the key regions and open and closed conformations of the flap of BACE1.

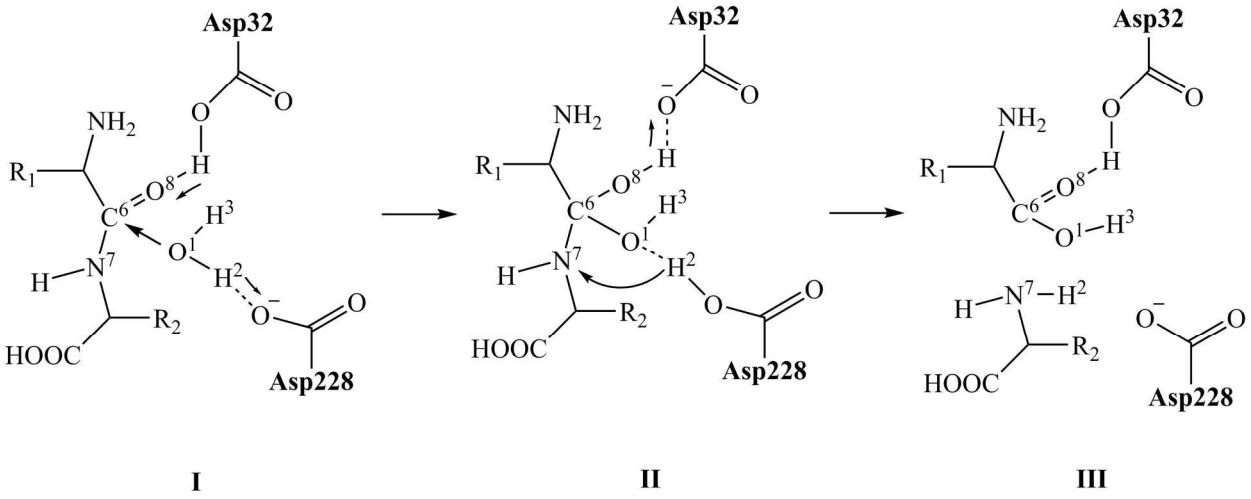

Figure 3: General acid/base mechanism utilized by BACE1 and other aspartyl proteases.

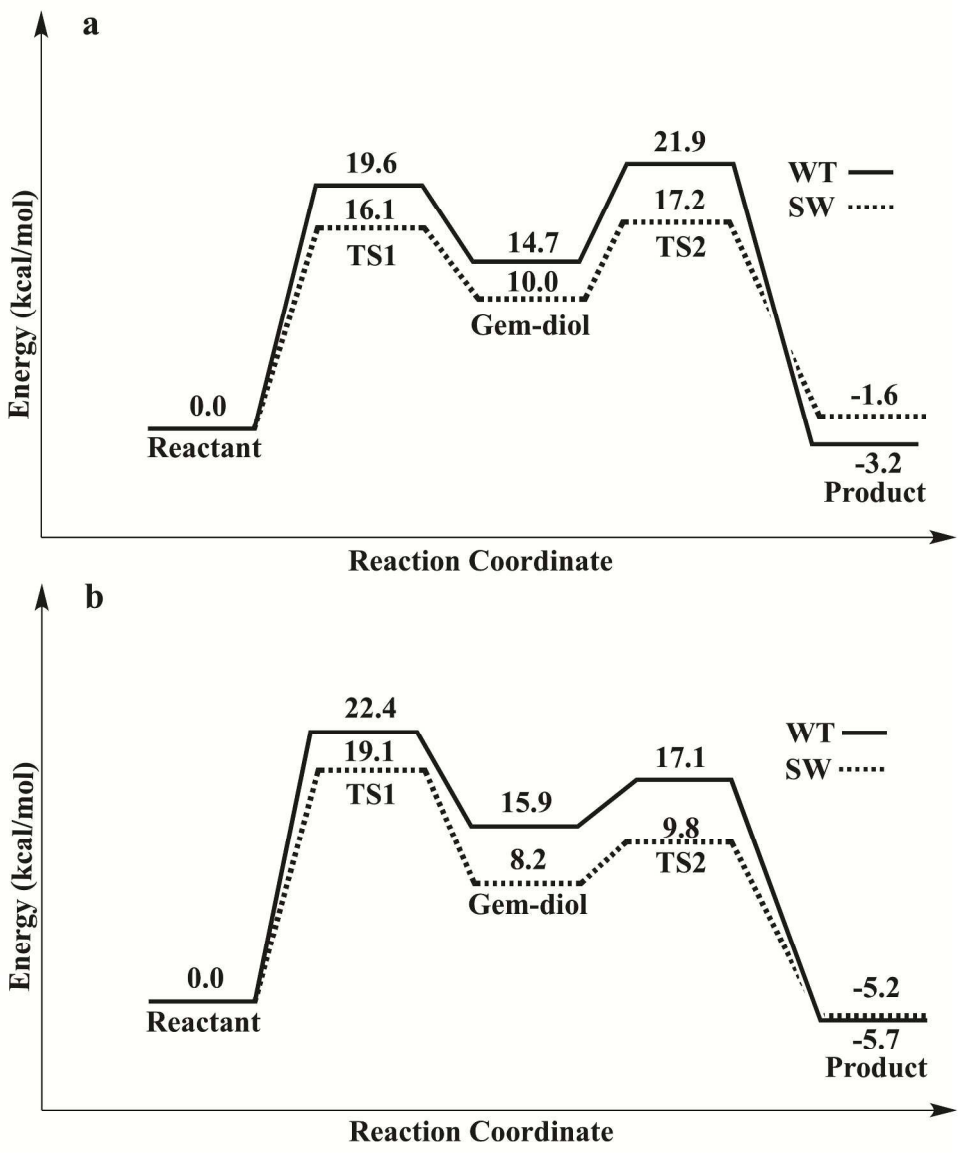

Figure 4: (a) Computed energetics of the mechanism of BACE1 at the QM level. **(b)** Computed energetics of the mechanism of BACE1 at the QM/MM level.

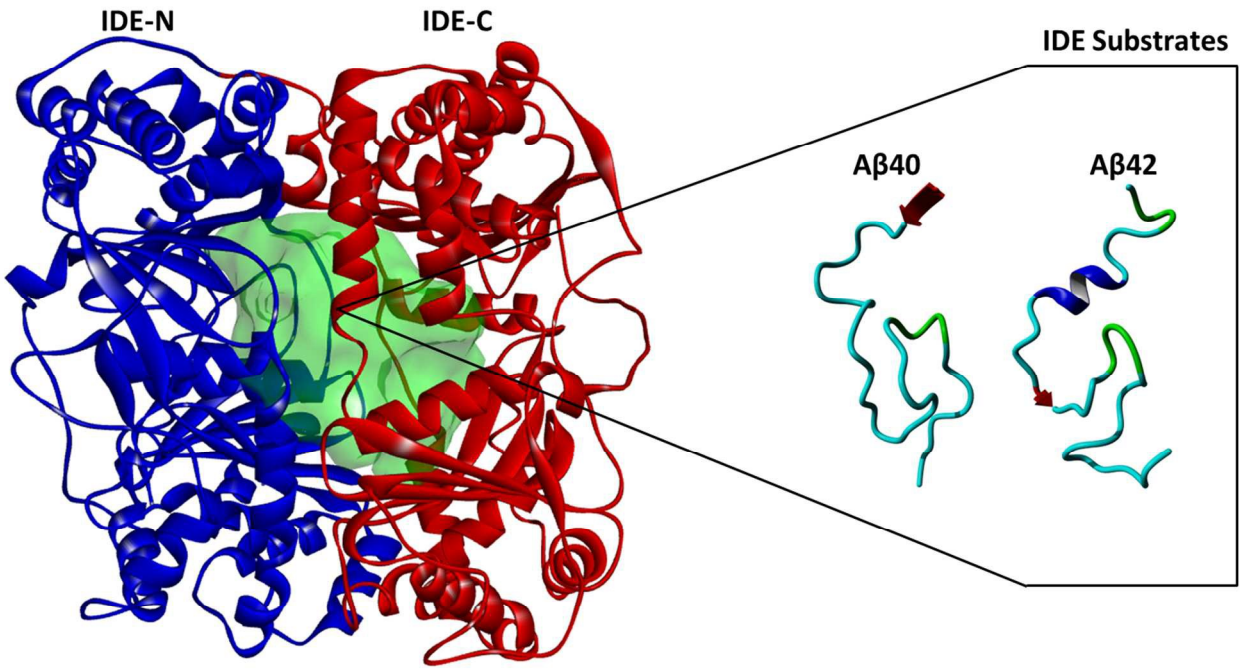

Figure 5: Structures of IDE and Aβ40 and Aβ42 substrates

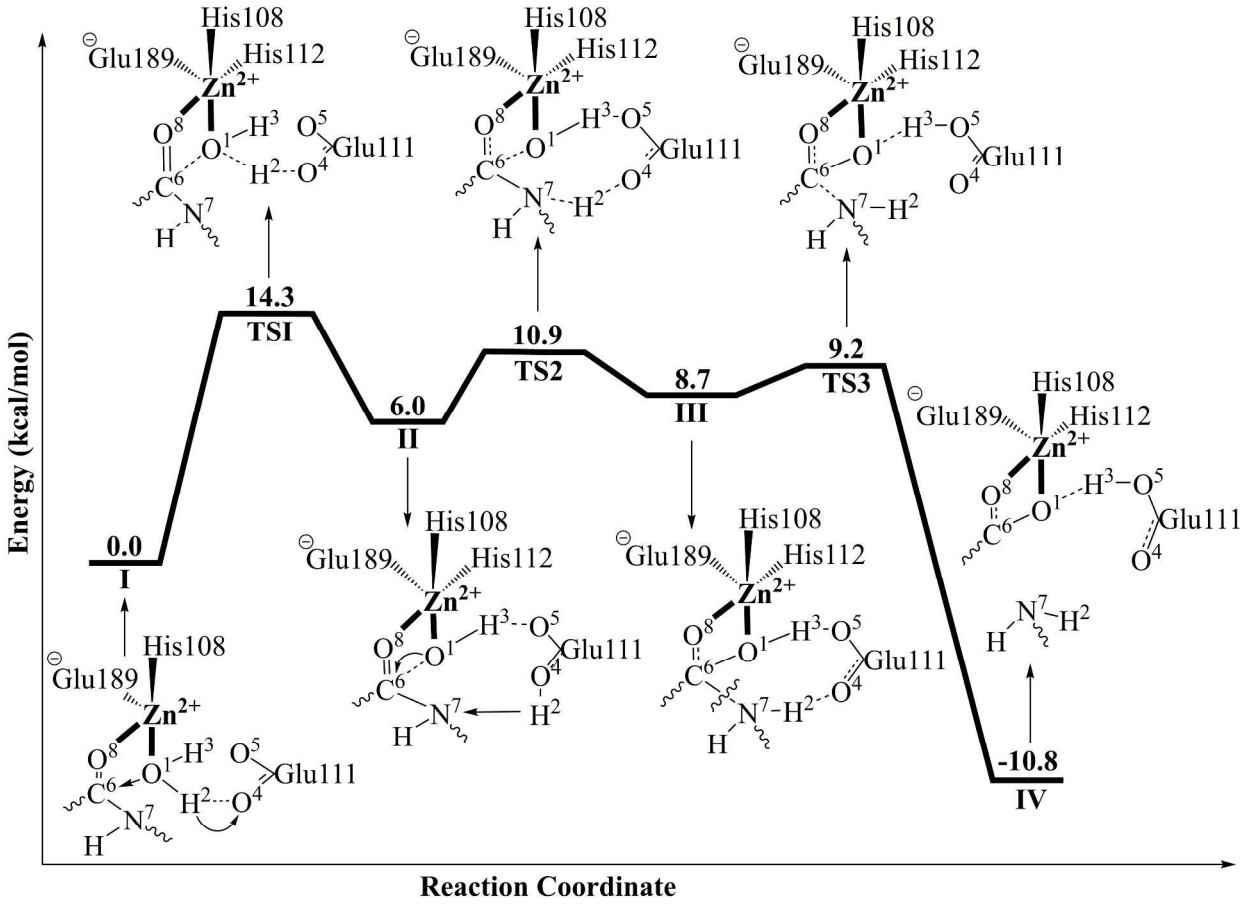

Figure 6: Mechanism and energetics of the hydrolysis of the Lys-Gly bond of IDE. The arrows in the figure describe the movement of atoms.

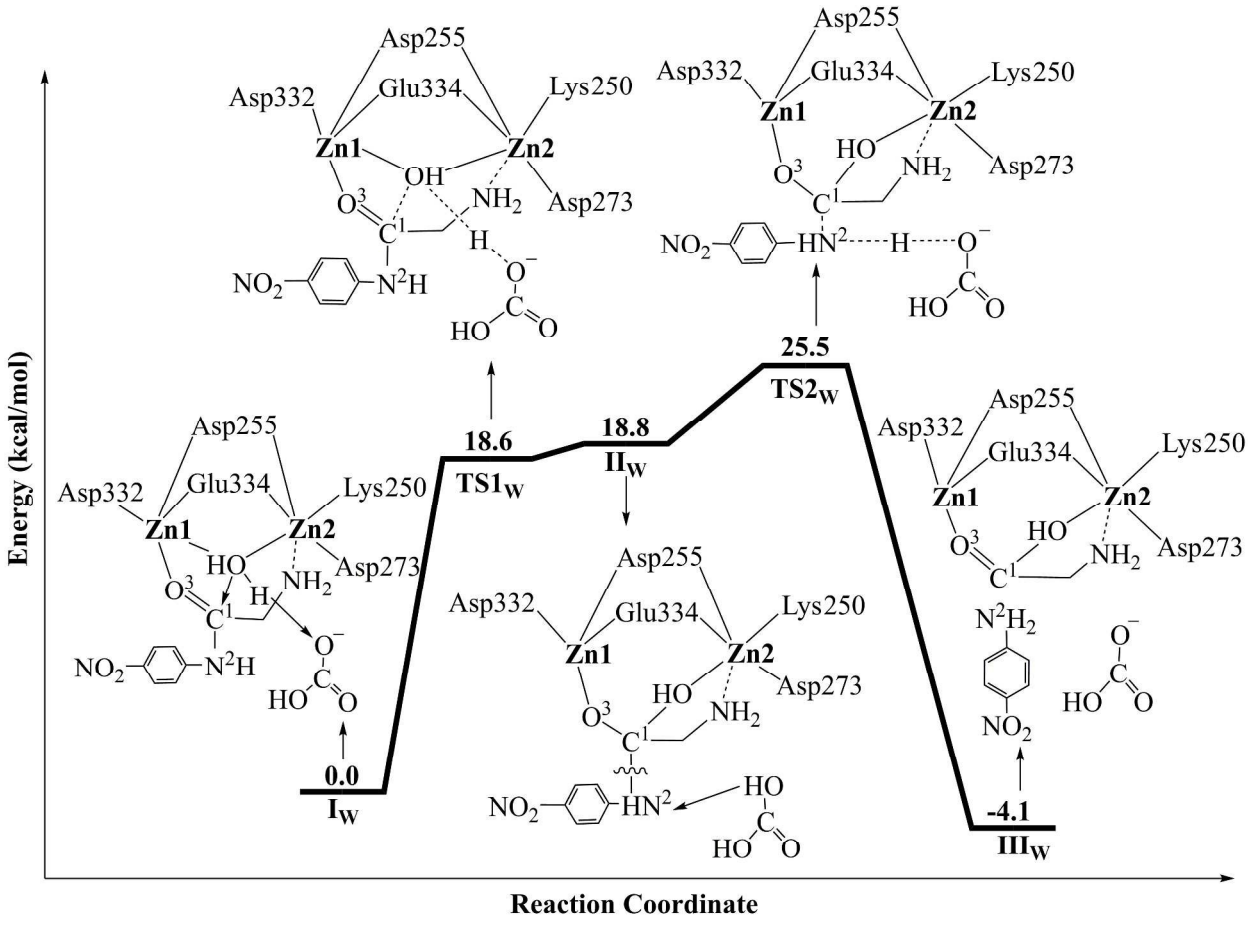

Figure 7a: Mechanism and energetics of BILAP using the water nucleophile. The arrows in the figure describe the movement of atoms.

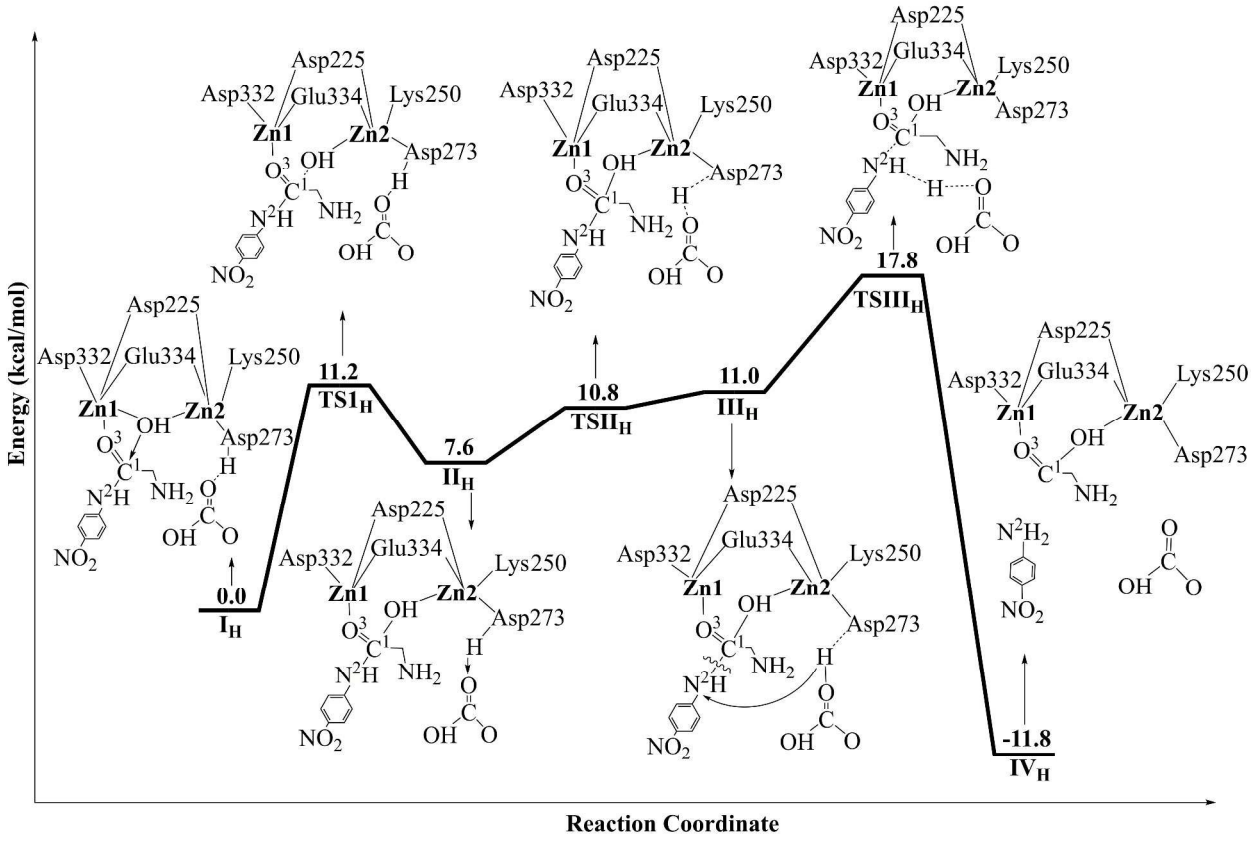

Figure 7b: Mechanism and energetics of BILAP using the hydroxyl nucleophile. The arrows in the figure describe the movement of atoms.

Table 1. Energy Barriers for Hydrolysis of the Phe−Phe bond by BACE1, IDE and MMP

Catalyst	**Barrier (kcal/mol)**
MMP	17.5
BACE1	22.5
IDE	24.4

Table of content (TOC) figure

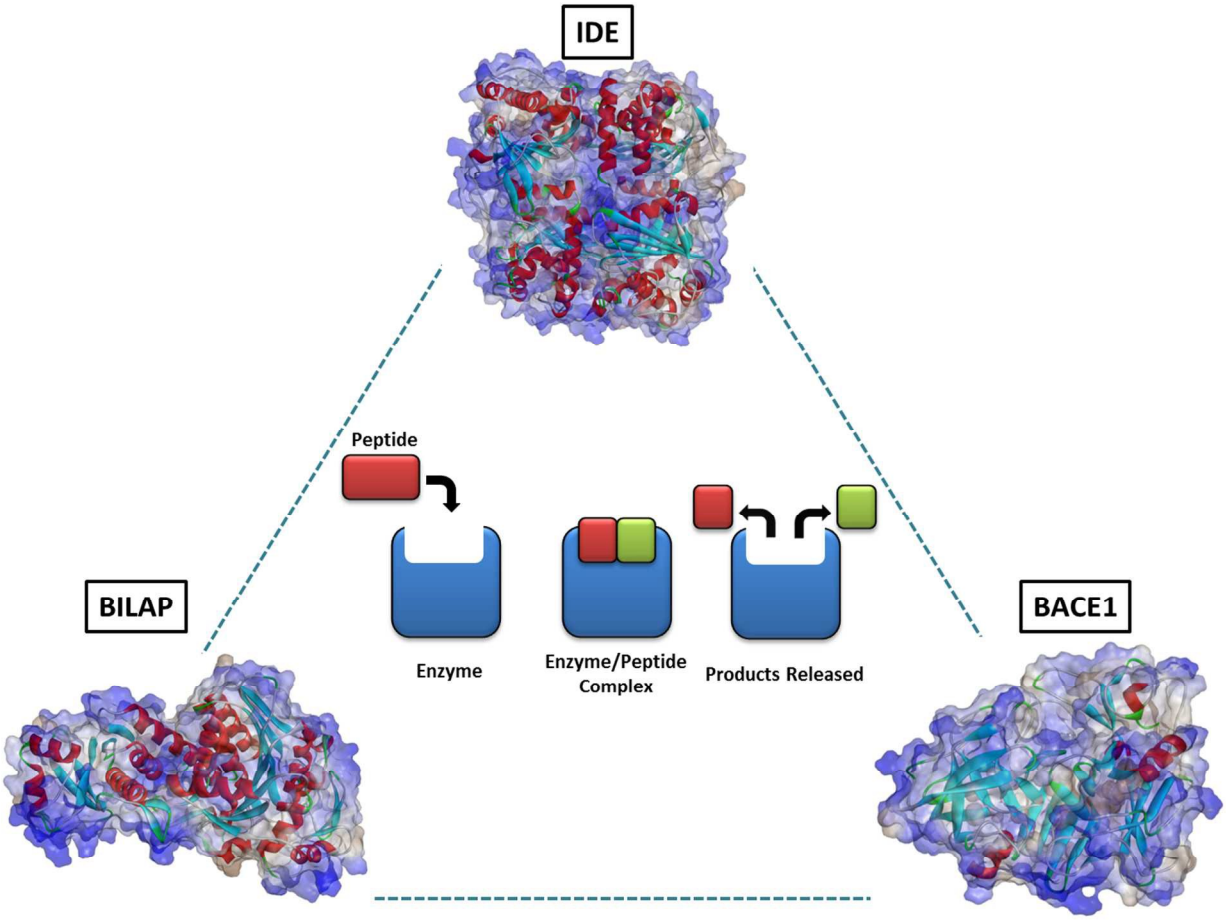

Biography

Thomas J. Paul received a B.A. in chemistry from Florida Gulf Coast University, Fort Myers, Florida in 2013. His research in the laboratory of Dr. Rajeev Prabhakar at the University of Miami, FL, U.S.A. is focused on the mechanistic, structural, and mechanical aspects of proteases and peptidases.

Arghya Barman received a M.S. in Biochemistry from the University of Calcutta, India in 2005. He received his Ph.D in the laboratory of Dr. Rajeev Prabhakar at the University of Miami, FL, U.S.A. in 2012. He is currently a postdoctoral fellow in Dr. Donald Hamelberg's lab at Georgia State University. His current research interests include investigations of molecular interactions and information transfer in complex biomolecular system.

Mehmet Ozbil received his B.S. from Istanbul Technical University, Istanbul, Turkey in 2007. He received his Ph.D in the laboratory of Dr. Rajeev Prabhakar at the University of Miami, FL, U.S.A. in 2013. He is currently assistant professor *İstanbul Arel Üniversitesi, Istanbul, Turkey*.

Ram Prasad Bora received his M.S. in physical chemistry from Andhra University, Andhra Pradesh, India. From 2008-2010, he did postdoctoral research training in the laboratory of Dr. Rajeev Prabhakar at the University of Miami, Miami, Florida, U.S.A. He is currently a postdoctoral fellow in Dr. Arieh Warshel's lab at the University of Southern California, U.S.A. His current research interests include exploring and understanding enzyme evolutionary aspects.

Tingting Zhang obtained her Ph.D in the laboratory of Dr. Rajeev Prabhakar at the University of Miami, FL, U.S.A. She is currently assistant professor in school of pharmaceutical sciences of Southern Medical University, Guangzhou city, China.

Gaurav Sharma obtained his Bachelor of Pharmacy from India, in 2011. He received his M.S. in pharmaceutical science from Idaho State University in 2014. His research in the laboratory of Dr. Rajeev Prabhakar at the University of Miami, FL, U.S.A. is focused on mechanistic properties of metallopeptidases.

Zachary Hoffmann received a B.A. in chemistry from Florida Gulf Coast University, Fort Myers, Florida in 2013. His research in the laboratory of Dr. Rajeev Prabhakar at the University of Miami, FL, U.S.A. is focused on the mechanistic aspects of proteases and peptidases.

Rajeev Prabhakar is an associate professor at the University of Miami, FL, U.S.A. in the department of chemistry. His main research interests are applications of innovative theoretical and computational approaches to study mechanisms of chemical and biochemical reactions, the design of catalysts, computer aided drug design and chemistry associated with neurological disorders.